molecular pharmaceutics

Article

pubs.acs.org/molecularpharmaceutics

Efficient Delivery of Sticky siRNA and Potent Gene Silencing in a Prostate Cancer Model Using a Generation 5 Triethanolamine-Core PAMAM Dendrimer

Xiaoxuan Liu,[†,#,‡] Cheng Liu,[#] Erik Laurini,[§] Paola Posocco,[§] Sabrina Pricl,[§] Fanqi Qu,[#] Palma Rocchi,[‡] and Ling Peng[†,*]

[†] Département de Chimie, Centre Interdisciplinaire de Nanoscience de Marseille, CNRS UMR 7325, Aix-Marseille Université, 163 avenue de Luminy, 13288 Marseille, France

[#]State Key Laboratory of Virology, College of Chemistry and Molecular Sciences, Wuhan University, Wuhan, 430072, P. R. China

[‡]Centre de Recherche en Cancérologie de Marseille, UMR1068 Inserm, Institut Paoli-Calmettes, Aix-Marseille Université, France

[§]Molecular Simulation Engineering (MOSE) Laboratory, Department of Industrial Engineering and Information Technology (DI3), University of Trieste, Via Valerio 10, 34127 Trieste, Italy

Supporting Information

ABSTRACT: Successful achievement of RNA interference in therapeutic applications requires safe and efficient vectors for siRNA delivery. In the present study, we demonstrate that a triethanolamine (TEA)-core PAMAM dendrimer of generation 5 ($\mathbf{G_5}$) is able to deliver sticky siRNAs bearing complementary A_n/T_n 3′-overhangs effectively to a prostate cancer model *in vitro* and *in vivo* and produce potent gene silencing of the heat shock protein 27, leading to a notable anticancer effect. The complementary A_n/T_n (n = 5 or 7) overhangs characteristic of these sticky siRNA molecules help the siRNA molecules self-assemble into "gene-like" longer double-stranded RNAs thus endowing a low generation dendrimer such as $\mathbf{G_5}$ with greater delivery capacity. In addition, the A_n/T_n (n = 5 or 7) overhangs act as protruding molecular arms that allow the siRNA molecule to enwrap the dendrimer and promote a better interaction and stronger binding, ultimately contributing toward the improved delivery activity of $\mathbf{G_5}$. Consequently, the low generation dendrimer $\mathbf{G_5}$ in combination with sticky siRNA therapeutics may constitute a promising gene silencing-based approach for combating castration-resistant prostate tumors or other cancers and diseases, for which no effective treatment currently exists.

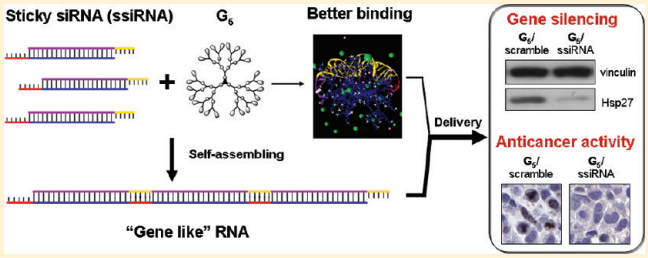

KEYWORDS: *dendrimer, sticky siRNA, siRNA delivery, gene silencing, Hsp27, prostate cancer*

INTRODUCTION

The promise that small-interfering RNAs (siRNAs) can efficiently and specifically downregulate genes with known sequence brings new hope for treating various important diseases.[1−3] However, the successful implementation of siRNA-based therapeutics requires safe and efficient siRNA delivery.[4] Although viral vectors are very effective for this purpose, the increasing concerns over their safety and the high costs relating to their complicated manipulation substantiate the need to develop alternative, nonviral vectors. We have recently demonstrated that the structurally flexible triethanolamine (TEA)-core poly(amidoamine) (PAMAM) dendrimers (Figure 1)[5,6] are excellent nonviral vectors for siRNA delivery both *in vitro* and *in vivo*.[7−10] Of particular interest, the generation 7 dendrimer ($\mathbf{G_7}$) can mediate efficient siRNA delivery and produce potent gene silencing of the heat shock protein 27 (Hsp27) leading to effective anticancer activity in a castration-resistant prostate cancer model.[8] Hsp27, an ATP-independent molecular chaperone involved in drug resistance, is considered as an attractive novel therapeutic target for treating castration-resistant prostate cancer,[11,12] for which there is currently no effective treatment.[13] Thus, a RNAi-based strategy to target Hsp27 using siRNA in combination with our TEA-core dendrimer $\mathbf{G_7}$ might constitute a promising new solution for prostate cancer treatment.[8] Importantly, it should be mentioned that the large-scale synthesis of the good quality TEA-core dendrimer $\mathbf{G_7}$ is particularly challenging. This is due to the seemingly easy but rather time-consuming and meticulous control of the reaction conditions as well as the tedious procedures of purifying the resulting, high generation PAMAM dendrimers. Accordingly, the possibility of developing low generation dendrimers for the effective delivery of siRNA

Special Issue: Biological Applications of Dendrimers

Received: November 29, 2011
Revised: December 24, 2011
Accepted: December 30, 2011
Published: December 30, 2011

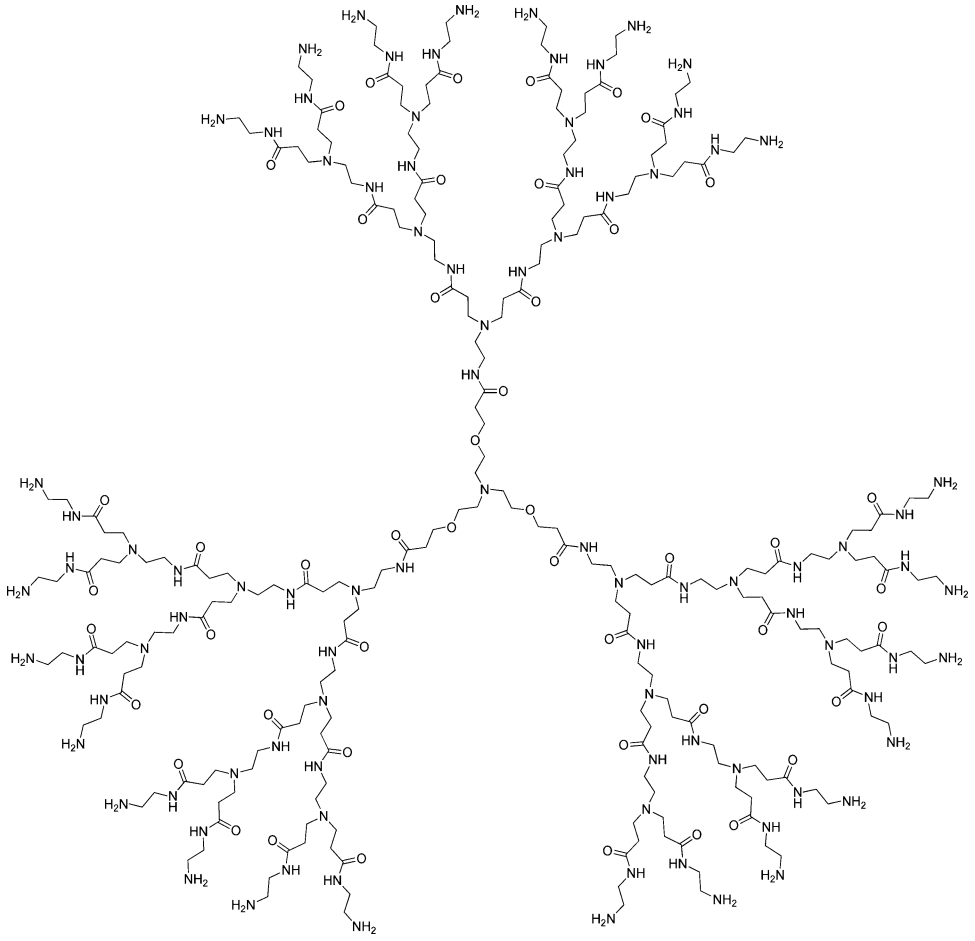

Figure 1. Chemical structure of triethanolamine (TEA) core PAMAM dendrimer. For clarity, only $\mathbf{G_3}$ is presented.

therapeutics constitutes *per se* a challenging but worthwhile goal.

Recently, Behr et al. reported that siRNAs with short complementary A_n/T_n (n = 5−8) 3′ overhangs, named "sticky" siRNA (Scheme 1A), could dramatically increase gene silencing efficiency when using polyethylenimine (PEI) as the delivery vector.[14] PEI is one of the best nonviral DNA delivery vectors,[15] but its efficiency drops considerably when delivery of conventional siRNA is concerned. This can be ascribed to the small size of the conventional siRNA, the binding cooperativity of which is insufficient to ensure the strong electrostatic interaction with the positively charged PEI vector required for effective delivery. The reason why PEI is able to efficiently deliver sticky siRNA can be explained by the presence of the complementary A_n/T_n overhangs on such sticky siRNAs which can self-assemble into "gene-like" long double-stranded RNA (Scheme 1B), allowing their successful delivery into cells by PEI with a mechanism similar to that presiding over plasmid DNA delivery.[14] These results reminded us of our earlier study on the importance of size-to-charge ratio in the construction of stable and uniform nanoscale RNA/dendrimer complexes,[16] where the size of the RNA molecules and the generation of the dendrimers both played a critical role. Indeed, higher generation dendrimers are required for a better interaction and efficient delivery of smaller siRNA molecules,[7,16] whereas lower generation dendrimers may be sufficient to allow a strong interaction with larger RNA molecules.[16]

Based on our earlier findings of the size effects on RNA/dendrimer complex formation and the recently reported sticky siRNA concept by Behr et al.,[14,16] we reasoned that, by using sticky siRNAs, we might be able to achieve efficient gene silencing using a dendrimer of lower generation than the effective $\mathbf{G_7}$ vector. Here, we report that a lower generation dendrimer, a TEA-core PAMAM dendrimer of generation 5 ($\mathbf{G_5}$), is indeed effective at delivering sticky siRNA into drug-resistant prostate cancer PC-3 cells, leading to potent gene silencing of Hsp27 and promising anticancer activity in a prostate cancer xenograft mouse model.

■ EXPERIMENTAL SECTION

Materials. The triethanolamine-core PAMAM dendrimers were synthesized as previously described.[5−8,16] The sequence of conventional Hsp27 siRNA used corresponded to the human Hsp27 site (5′-GCUGCAAAAUCCGAUGAGACdTdT-3′; Dharmacon, Lafayette, CO). A scrambled siRNA duplex (5′-AUCAAACUGUUGUCAGCGCUGdTdT-3′) was used as a control. The 25 and 27 mer Hsp27 sticky siRNAs used the same target sequence as conventional siRNA with complementary A_5/T_5 overhanged at the 3′ end (sense, 5′-GCU GCA AAA UCC GAU GAG AC dAdAdAdAdA-3′; antisense, 5′-GUC UCA UCG GAU UUU GCA GC dTdTdTdTdT-3′) or A_7/T_7 at the 3′ end (sense, 5′-GCU GCA AAA UCC GAU GAG AC dAdAdAdAdAdAdA-3′; antisense, 5′-GUC UCA UCG GAU UUU GCA GC dTdTdTdTdTdTdT-3′), and the sequences of the relevant scrambled sticky siRNAs are as follows: 25 mer

dx.doi.org/10.1021/mp2006104 | *Mol. Pharmaceutics* 2012, 9, 470−481

Scheme 1. Cartoon Presentation of Conventional siRNA and Self-Assembly of Sticky siRNA[a]

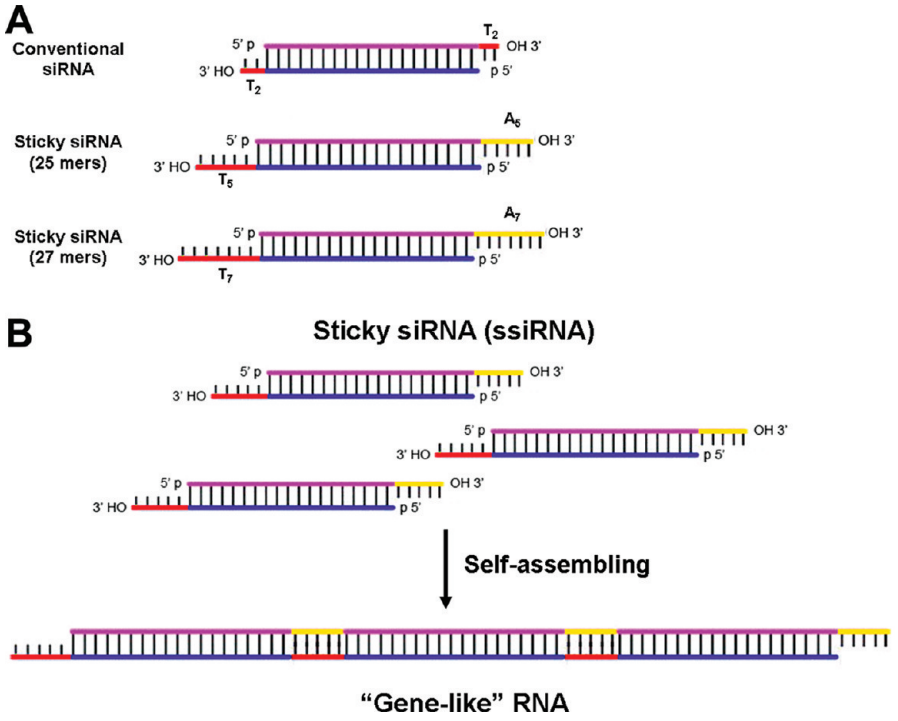

[a](A) Cartoon presentation of conventional siRNA with T_2/T_2 3′ overhangs (22 mer siRNA), and sticky siRNA molecules with A_n/T_n 3′ overhangs. The sticky siRNAs used in this study are named as 25 and 27 mer stick siRNAs with n = 5 and 7, respectively. (B) Self-assembly of sticky siRNA into "gene-like" longer double stranded RNA.

scramble sense, 5′-CUU ACG CUG AGU ACU UCG A dAdAdAdAdA-3′; antisense, 5′-UCG AAG UAC UCA GCG UAA G dTdTdTdTdT-3′; 27 mer scramble sense, 5′-CUU ACG CUG AGU ACU UCG A dAdAdAdAdAdAdA-3′; antisense, 5′-UCG AAG UAC UCA GCG UAA G dTdTdTdT-dTdTdT-3′. All the above sticky siRNAs together with 5′-Alexa647 labeled sticky siRNAs were purchased in Eurogentec. Ethidium bromide, endocytosis inhibitors (cytochalasin D, genistein and chlorpromazine), paraformaldehyde, and bovine serum albumin (BSA) were supplied by Sigma (Sigma-Aldrich, Lyon, France). Endocytic markers (Alexa-Fluor 488-labeled dextran, transferrin, and cholera toxin B), Alexa-Fluor 647-labeled phalloidin, 4′,6′-diamidino-2-phenylindole (DAPI) and Hoechst 34580 were purchased from Invitrogen (Invitrogen Ltd., Paisley, U.K.). All other reagents and solvents of analytical grade were used without further purification from commercial sources.

Molecular Modeling. All MD simulations were performed using the *sander* and *pmemd* modules of the AMBER 9 suite of programs,[17] The AMBER ff03 force field (FF)[17] and the new version of the Dreiding FF recently developed by the Goddard group and specifically optimized for dendrimers in water solutions[17] were employed for the nucleic acid and the dendrimers, respectively. The free energy of binding between the dendrimers and the siRNAs was calculated according to a previously validated approach[18,19] based on the Molecular Mechanics/Poisson−Boltzmann surface area (MM/PBSA) methodology.[20] Calculations were carried out in parallel on 128 processors of IBM/SP6 calculation cluster of the CINECA supercomputer facility (Bologna, Italy).

Size and Zeta Potential Measurement of Sticky siRNA/G_5 Complexes. The sticky siRNA solution was mixed with indicated amount of the dendrimer G_5 solution at N/P ratio 10. The final concentration of the sticky siRNA was 1 μM. After incubation at 37 °C for 30 min, size and zeta potential measurements were performed using Zetasizer Nano-ZS (Malvern, Ltd. Malvern, U.K.) with a He−Ne ion laser of 633 nm.

Stability of Sticky siRNA/Dendrimer Complex against RNaseA. An aliquot of 2.2 μg of sticky siRNA and the indicated amounts of G_5 at N/P (= [total terminal amines in G_5]/[phosphates in siRNA]) ratio 10 was kept at 37 °C for 30 min. Then the complexes were incubated in the presence of 0.01 μg/μL RNase A for 0, 5, 10, 15, 20, 30, 45, 60, 75, 90, and 120 min at 37 °C. Aliquots (4 μL) of the corresponding solution were withdrawn, added to 1.5 μL of 1% SDS solution on the ice and then subjected to electrophoresis in 1.2% agarose gel in standard TBE buffer. The sticky siRNA bands were stained by ethidium bromide and then detected by a Herolab EASY CCD camera (type 429K) (Herolab, Wiesloch, Germany).

Cell Culture. Human prostate cancer PC-3 cells were purchased from the American Type Culture Collection (Manassas, VA). Cells were maintained in DMEM (Lonza Group Ltd., Switzerland), supplemented with 10% fetal bovine serum (FBS). Cells were maintained at 37 °C in a 5% CO_2 humidified atmosphere.

Uptake of Sticky siRNA/G_5 Complexes in PC-3 Cells. To evaluate cellular uptake and subsequent intracellular routing of complexes, Alexa647 labeled Hsp27 sticky siRNA (25 mer) was used. One day before use, PC-3 cells were seeded at a density of 10×10^4 cells/chamber in 4-well glass chamber slides (Lab-Tek, Nunc, USA). Preparation of the sticky siRNA/G_5 complexes was performed as indicated above. Then, the complex containing Alexa647-labeled sticky siRNA was added to the cells in Opti-MEM transfection medium.

Confocal Microscopy. After 4 h incubation at 37 °C, the cells were washed with PBS and stained with Hoechst 34580. A Zeiss LSM 510 Meta laser scanning confocal microscope equipped with inverted Zeiss Axiovert 200 M stand (Carl Zeiss GmbH, Jena, Germany) was used for visualization. Images were acquired using LSM 510 software (Carl Zeiss GmbH, Jena, Germany). For cell uptake in the presence of endocytic markers, the Alexa-Fluor 488-labeled markers were added during the final 30 min incubation of sticky siRNA/$\mathbf{G}_5$ nanoparticles prior to nuclear staining with Hoechst. For observation of actin rearrangement, after incubation for 15 min at 37 °C with sticky siRNA/$\mathbf{G}_5$ nanoparticles, cells were fixed in 4% paraformaldehyde, permeabilized with 0.1% triton, incubated with 1% bovine serum albumin (BSA) and stained with Alexa-Fluor 647 phalloidin to label actin fibers, then with DAPI to label the nuclei.

Flow Cytometry. The uptake mechanism of the sticky siRNA/$\mathbf{G}_5$ nanoparticles was examined by means of specific inhibitors of different endocytic pathways. For inhibition experiments, the cells were seeded at a density of 3×10^5 cells in 3.5 cm dishes (Nunc, USA) one day before, and then they were incubated with one of the following inhibitors: cytochalasin D (to inhibit macropinocytosis), genistein (to inhibit caveolae-mediated endocytosis), or chlorpromazine (to inhibit clathrin-mediated endocytosis) for 1 h in completed medium before the sticky siRNA/$\mathbf{G}_5$ complexes were added. Inhibitors were used at concentrations in which they were not cytotoxic for PC-3 cells. After incubation for 15 min at 37 °C with Alexa647-labeled sticky siRNA/$\mathbf{G}_5$ complex, the cell uptake efficiency was measured using flow cytometry analysis (Beckman Coulter Epics Elite, Beckman Inc., Miami, FL). Each assay was performed in triplicate.

***In Vitro* Transfection Experiments.** One day before transfection, 1.5×10^5 cells were seeded in 6 cm dishes in 4 mL of fresh complete medium containing 10% FBS. Before transfection, a solution of the sticky siRNA/$\mathbf{G}_5$ complex was prepared accordingly. The desired amount of sticky siRNA and $\mathbf{G}_5$ was diluted in 200 μL of Opti-MEM tranfection medium. The solutions were mixed with a vortex for 10 s and then left for 10 min at room temperature. The dendrimer $\mathbf{G}_5$ was added to the sticky siRNA solution, homogenized for 10 s with a vortex and left 30 min at room temperature. Then 1.6 mL of serum-free medium was added into the complex solution and the final volume brought to 2 mL. Before addition of the transfection complexes, the complete medium with serum was removed and cells were washed with PBS once. Then, 2 mL of complex solution was added and incubated at 37 °C in the absence of 10% fetal bovine serum. After 8 h of incubation, the transfection mixture was replaced with the complete medium containing 10% fetal bovine serum (FBS), and maintained under normal growth conditions for further incubation of 48 or 72 h.

Quantitative Real-Time (qRT)-PCR. The expression of the Hsp27 mRNAs was analyzed by quantitative real-time PCR amplification analysis. Total RNAs were isolated using the Trizol method (Invitrogen). Then 1 μg of RNAs was reverse-transcribed into cDNA by using ImProm-II Reverse Transcription system (Promega) (0.5 μg of oligo dT primer, 1 μL of ImProm-II reverse transcriptase, 0.5 μL of RNase inhibitor, 1 μL of 10 mM dNTP mix, 4.8 μL of 25 mM $MgCl_2$, 4 μL of 5× RT buffer) in a final volume of 20 μL. The thermal cycling protocol employed included two steps (step 1, 70 °C for 5 min, and 4 °C for 5 min; step 2, 25 °C for 5 min, 42 °C for 1 h, 70 °C for 15 min, and 4 °C forever).

The real-time PCR was conducted using the LightCycler 2.0 instrument (Roche Diagnostics, GmbH Mannheim, Germany). Reaction mixtures contained total volume of 20 μL consisting of 5 μL of each diluted cDNA (1:10), 10 μL of SYBR Premix Ex Taq (2×) (TaKaRa Bio. Inc., Japan), 0.4 μL of primers F and primers R (10 μM) of target gene Hsp27 and internal control 18S, and 4.2 μL of H_2O. The sequences of primers are as follows: Hsp27 primer F, 5′-TCCCTGGATGTCAACCACTTC-3′, and primer R, 5′-TCTCCACCACGCCATCCT-3′; 18S primer F, 5′-CTACCACATCCAAGGAAGGC-3′, and primer R, 5′-TTTTCGTCACTACCTCCCCG-3 (Eurogentec S. A., Seraing, Belgium). The conditions were as follows: an initial denaturation step at 95 °C for 10 s; then 45 cycles of 95 °C for 5 s, 57 °C for 6 s, and 72 °C for 12 s. A melting curve was carried out after an amplification program by heating at temperatures from 65 to 95 °C in 1.5 min. A final cooling step at 40 °C for 1 min was performed. Each sample was analyzed in triplicate in the PCR reaction to estimate the reproducibility of data. The data was acquired by using Roche Molecular Biochemicals light cycler software version 3.5, and statistical analysis was obtained by RelQuant (Roche).

Western Blot Analysis. Samples containing equal amounts of protein (15 μg) from lysates of cultured PC-3 cells or tumors were analyzed by Western blot analysis as described previously[21] with 1:5000-diluted anti-human Hsp27 rabbit polyclonal antibody (Stressgen Assay Designs Inc., Ann Arbor, MI, USA) or 1:2000-diluted anti-human vinculin mouse monoclonal antibody (Sigma Chemical Co., St. Louis, MO). Filters were then incubated for 1 h at room temperature with 1:5000-diluted horseradish peroxidase conjugate anti-rabbit or mouse monoclonal antibody (Santa Cruz Biotechnology, Inc., Santa Cruz, CA). Specific proteins were detected using an enhanced chemiluminescence Western blotting analysis system (Amersham Life Science, Arlington Heights, IL).

MTT (3-(4,5-Dimethylthiazol-2-yl)-2,5-diphenyl Tetrazolium Bromide) Assay. The growth inhibitory effects of Hsp27 sticky siRNA plus $\mathbf{G}_5$ on PC-3 cells were assessed using the 3-(4,5-dimethylthiazol-2-yl)-2,5-diphenyltetrazolium bromide (MTT) assay (Sigma-Aldrich, Lyon, France). Briefly, cells were seeded in each well of 12-well microtiter plates and allowed to attach overnight. Cells were then treated once daily with sticky siRNA/$\mathbf{G}_5$ for 8 h. Every 24 h over a period of 7 days, MTT assays were carried out. Each assay was performed in triplicate.

Apoptosis (Annexin V Assay) by FACS Analysis. The PC-3 cells were plated into 6 cm dishes, and treated with Hsp27 sticky siRNA/$\mathbf{G}_5$ and scramble/$\mathbf{G}_5$ using no treatment and $\mathbf{G}_5$ alone as controls. Following treatment, the cells were trypsinized 4 days after treatment, washed twice with cold PBS buffer, resuspended in 100 μL binding buffer (1×) and transferred to a 500 μL culture tube.

Five microliters of annexin V-PE and 0.5 μL of 7-AAD (7-aminoactinomycin D) were added to each tube. Cells were gently vortexed and incubated for 15 min at room temperature (25 °C) in the dark. Next, 100 μL of binding buffer (1×) (10 mM HEPES, 140 mM NaCl, 2.5 mM $CaCl_2$, pH 7.4) was added to each tube and the cell suspension was subsequently analyzed by flow cytometry. Data was acquired on a fluorescence activated cell sorting (FACS Calibur, Becton Dickinson, Le Pont-De-Claix, France) using CellQuest software and analyzed by FlowJo software (Tree Star, Inc.). Ten thousand cells

were analyzed for each sample. Each assay was performed in triplicate.

Measurement of Caspase-3 Cleavage and Activity. Caspase-3 cleavage was detected by Western blotting as described above using 100 μg of protein. Polyclonal antibody (Cell Signaling Technology, Inc., Beverly, MA, USA) was used to detect full-length (M_r 32,000 to 35,000) and large fragment of activated caspase-3 (M_r 17,000 to 20,000) that results from cleavage after Asp175.

Caspase-3 activity was analyzed using Caspase-Glo 3/7 assay luminescent kit (Promega) or the Apo-ONE homogeneous caspase-3/7 assay fluorometric kit (Promega). PC-3 cells were seeded in each well of 96-well microtiter plates and allowed to attach overnight. Cells were then treated once daily with sticky siRNA/$\mathbf{G_5}$ for 8 h in the absence of 10% fetal bovine serum. Every 24 h over a period of 3 days, caspase-3 activity was measured by the cleavage of the luminogenic substrate containing the DEVD sequence or the fluorometric substrate Z-DEVD-R110 according to the instructions of the manufacturer (Promega). Next 100 μL of Caspase-Glo 3/7 reagent was added to each well of a white 96-well plate containing 100 μL of blank control, or cells in culture. The plate was covered with a plate sealer and incubated at room temperature for 1 h before the luminescence of each well was measured. Each experiment was performed in triplicate.

Lactate Dehydrogenase (LDH) Assay. PC-3 cells were seeded by 5000 cells per well in 96-well plates and cultured overnight. The cells were treated with sticky siRNA/$\mathbf{G_5}$ for 8 h in the absence of 10% fetal bovine serum. After 1, 3, and 24 h, the LDH concentration was measured by using commercial LDH kit (Cytotoxicity Detection Kit, Roche). The LDH reaction mixture was freshly prepared according to the manufacturer's protocol (Roche Diagnostics), 100 μL added to each well of a 96-well plate containing 100 μL of blank, control, or cells in culture, and the plate incubated for 30 min at 25 °C. Control was performed with lysis buffer and medium, and set as 100% and 0% LDH release, respectively. The relative LDH release is defined by the ratio of LDH released over total LDH in the intact cells. All samples were run in triplicate.

Assessment of *in Vivo* Gene Silencing and Apoptosis. Institutional guidelines for the proper and humane use of animals in research were followed. Approximately 10×10^6 PC-3 cells were inoculated subcutaneously with 0.1 mL of DMEM (Lonza Group Ltd., Switzerland) which was supplemented with 10% FBS in the flank region of 5-week-old male xenograft nude mice (Charles River Laboratories, France) via a 27-gauge needle. When PC-3 tumors reached 100 mm^3, usually 3 to 4 weeks after injection, mice were randomly selected for treatment with 25 mer Hsp27 sticky siRNA/$\mathbf{G_5}$, scramble/$\mathbf{G_5}$, Hsp27 sticky siRNA alone, $\mathbf{G_5}$ alone, or PBS buffer alone. Each experimental group consisted of 3 mice. After randomization, PBS buffer, 3 mg/kg Hsp27 sticky siRNA, $\mathbf{G_5}$ at N/P ratio = 5, Hsp27 sticky siRNA/$\mathbf{G_5}$ or scramble/$\mathbf{G_5}$ complexes, respectively, were injected intratumorally twice per week for one week. After one week of treatments, mice were sacrificed, and tumors were removed from the animals and divided into two parts. One part of the tumors was frozen in liquid nitrogen and then stored at −80 °C for RNA and protein extraction. The *in vivo* expression of Hsp27 mRNA and protein was measured, respectively, by qRT-PCR and Western blot as described before, as well as *in vivo* caspase activation. Another part of the tumors was fixed in 4% paraformaldehyde at 4 °C for immunohistochemistry.

Immunohistochemistry. Four-micrometer sections were dried overnight at 37 °C. Prior to antibody staining, the slides were pretreated with 10 mM citric acid (pH 6.0) for 20 min at 95 °C and 30 min at room temperature to unmask binding epitopes. After blocking of endogenous peroxidase activity with a 3% solution of hydrogen peroxide in PBS for 30 min, slides were washed thoroughly in water. After three washes in PBS, the slides were incubated with a 1:200 dilution of rabbit anti-Ki-67 monoclonal antibody (2746-1; Epitomics,Inc., Burlingame, CA, USA) in PBS for 1 h at room temperature. After three more washes in PBS, 1:400 dilution of biotinylated goat anti-rabbit (Ki-67) (E0432; Dako UK Ltd., Cambridgeshire, U.K.) in PBS was applied for 30 min at room temperature. After an additional three washes, streptavidin-HRP (P0397; Dako UK Ltd., Cambridgeshire, U.K.) was added for 30 min at room temperature. The staining was visualized by adding diaminobenzidine (DAB) (K3468; Dako UK Ltd., Cambridgeshire, U.K.) for 10 min at room temperature. The slides were washed well in water and counterstained with Mayers hematoxylin for 20 to 30 s, then washed in water again and topped in 0.1% Na_2CO_3 for 3 min, and then dehydrated, cleared, and mounted in distyrene plasticizer xylene (DPX). Positive and negative controls were performed with each batch of slides. Photomicrographs were taken through a Leica DMLS microscope coupled to a digital camera (Photometrics CoolSNAP, Roper Scientific, Inc., Glenwood, IL).

Statistical Analysis. Statistical analysis was performed by a one way ANOVA test followed by Fisher's protected least significant difference (PLSD) test (Statview 512, Brain Power Inc., Calabases, CA). $p \leq 0.05$ was considered significant (*); $p \leq 0.01$ (**); $p \leq 0.001$ (***).

RESULTS AND DISCUSSION

Lower Generation Dendrimer $\mathbf{G_5}$ Effectively Delivered Sticky siRNA into and Silenced Hsp27 within Prostate Cancer PC-3 Cells. We constructed two sticky siRNA molecules with complementary A_5/T_5 and A_7/T_7 3′ overhangs, respectively, to target Hsp27 (Scheme 1). They were named as 25 and 27 mer sticky siRNA (ssiRNA) accordingly. We then tested TEA-core PAMAM dendrimers from generations 4 to 7 ($\mathbf{G_4}$–$\mathbf{G_7}$) for their ability to deliver these two sticky siRNAs targeting Hsp27 in prostate cancer PC-3 cells (Figure 2A). To our great interest, dendrimers starting from generation 5 exhibited significant gene silencing with both 25 and 27 mer sticky siRNAs (Figure 2A). As we know from our previous study that $\mathbf{G_5}$ was unable to yield effective gene silencing in combination with conventional Hsp27 siRNA,[8] we hence concluded that the efficient gene silencing presently achieved with low generation dendrimer $\mathbf{G_5}$ was the direct consequence of the sticky siRNAs employed. A sensible molecular rationale for this finding is that the sticky siRNAs, via their A_5/T_5 or A_7/T_7 3′-overhangs, can self-assemble into "gene-like" longer double-stranded RNA molecules (Scheme 1B),[14] thus providing sufficient cooperativity and strong interactive forces with the small dendrimer $\mathbf{G_5}$, ultimately endowing it with good delivery capacity.

As $\mathbf{G_5}$ was the lowest generation dendrimer displaying effective activity for sticky siRNA delivery, we focused our attention on $\mathbf{G_5}$ for all further investigations. Additional optimization of the delivery conditions indicated that $\mathbf{G_5}$-mediated sticky siRNA delivery depends critically on both sticky siRNA concentration (Figure 2B) and the N/P charge ratio of $\mathbf{G_5}$ to sticky siRNAs (Figure 2C). The best gene silencing effect was obtained

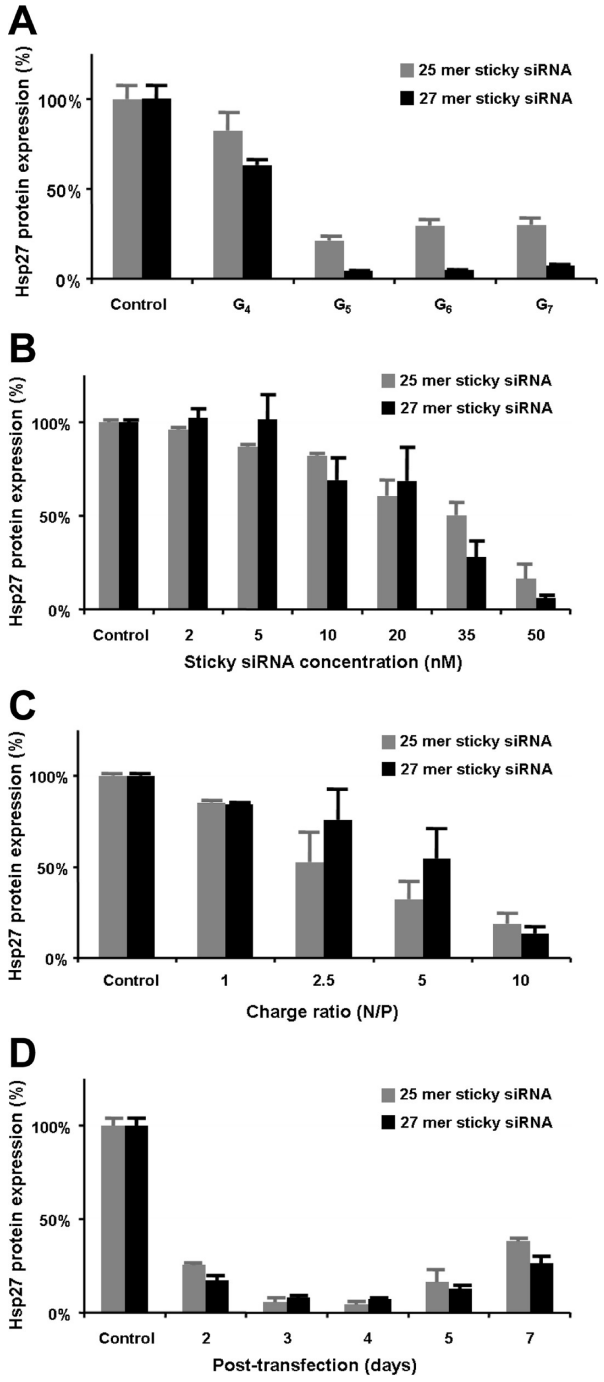

Figure 2. Dendrimer-mediated delivery of sticky siRNA to target heat shock protein 27 (Hsp27) in prostate cancer PC-3 cells. The expression of Hsp27 protein was assessed using Western blotting, with vinculin as reference. The resulting gene silencing depends on (A) dendrimer generation ($\mathbf{G_4}$–$\mathbf{G_7}$), (B) sticky siRNA concentration in combination with $\mathbf{G_5}$ and (C) charge ratio (N/P ratio) between $\mathbf{G_5}$ and sticky siRNA, and (D) has long-term effect.

with 50 nM sticky siRNAs at an N/P ratio of 10 for $\mathbf{G_5}$. Most importantly, the excellent gene silencing effect could be maintained even after 1 week post-treatment (Figure 2D), implying that the combination of $\mathbf{G_5}$/sticky siRNA is powerful enough to produce efficient and long-term gene silencing.

The Overhangs of Sticky siRNA Enhance the Binding Affinity with the Dendrimer $\mathbf{G_5}$. We further checked whether, in addition to the hypothesized formation of "gene-like" longer double strand RNA molecules,[14] the two complementary A_n/T_n (n = 5 or 7) overhangs of the sticky siRNAs might also behave as protruding molecular arms that allow the siRNA molecule to enwrap the spherical, low generation dendrimers with higher binding affinity than conventional siRNA with their two shorter T_2/T_2 overhangs. To this end, we studied the formation of a complex between $\mathbf{G_5}$ and different siRNA molecules (conventional siRNA with T_2/T_2 overhangs, and sticky siRNAs with either A_5/T_5 or A_7/T_7 overhangs) by computer modeling using atomistic molecular dynamics (MD) techniques. Figure 2 shows the MD snapshots of $\mathbf{G_5}$ in complex with siRNA bearing T_2/T_2 overhangs (Figure 3A), A_5/T_5 overhangs (Figure 3B), and A_7/T_7 overhangs (Figure 3C) at different time points along the MD trajectory. The structural differences between these complexes are blindingly obvious: both longer overhangs (A_5/T_5 and A_7/T_7) were found to significantly enhance the binding capacity of the sticky siRNAs to the $\mathbf{G_5}$ dendrimer allowing the formation of more compact complexes. In both these cases (Figure 3B and 3C), not only do the unpaired overhangs act as anchoring points for the siRNA onto the dendrimer surface but also the double-stranded portion of the siRNA molecule better adapts its overall conformation for a more efficient interaction with the $\mathbf{G_5}$ dendrimer. On the contrary, the presence of the short T_2/T_2 overhangs causes no substantial improvement of dendrimer binding by the relevant siRNA (Figure 3A). All these pictorial pieces of evidence are quantitatively substantiated by the corresponding values of the free energy of binding, ΔG_{bind}, between each siRNA and the $\mathbf{G_5}$ dendrimer, as estimated by the Molecular Mechanics/Poisson–Boltzmann surface area (MM/PBSA) analysis (Table 1). Indeed, the ΔG_{bind} values obtained for $\mathbf{G_5}$ and the sticky siRNAs with A_5/T_5 and A_7/T_7 overhangs are lower than that calculated for $\mathbf{G_5}$ and the conventional siRNA with T_2/T_2 overhangs (Table 1), indicating that the binding affinity of $\mathbf{G_5}$ for sticky siRNAs is higher than that for conventional siRNA. Based on these results, we hypothesized that, in addition to the possible formation of "gene-like" longer double-stranded RNA molecules,[14] the stronger binding to dendrimers of sticky siRNAs compared to conventional siRNA might also contribute to the enhanced delivery activity of $\mathbf{G_5}$.

$\mathbf{G_5}$ Form Stable Nanoparticles with Sticky siRNAs Which Promotes Cell Uptake. The positively charged dendrimer $\mathbf{G_5}$ is able to effectively compact the negatively charged sticky siRNAs into nanoparticles of around 100 nm, as demonstrated by the results obtained from dynamic light scattering analysis (Figure S1 and Table S1 in the Supporting Information). Further surface potential measurements showed that these nanoparticles had positive zeta potential values around +40 mV (Table S1 in the Supporting Information), indicating their colloidal stability. In addition, the $\mathbf{G_5}$/sticky siRNA complexes were found to effectively protect the sticky siRNAs against enzymatic degradation (Figure S2 in the Supporting Information). Collectively, these findings suggest that $\mathbf{G_5}$ dendrimers form stable nanoparticles with sticky siRNAs and can protect them from degradation, both very important properties for an effective delivery process.

As cell uptake is one of the initial steps of the delivery process, we next verified the internalization of the sticky siRNA/$\mathbf{G_5}$ dendrimer complexes into PC-3 cells using live-cell confocal microscopy with far-red fluorescent dye Alexa647-labeled sticky siRNA. Significantly prominent red fluorescent signals were observed in the cytoplasm when $\mathbf{G_5}$ was used

dx.doi.org/10.1021/mp2006104 | Mol. Pharmaceutics 2012, 9, 470–481

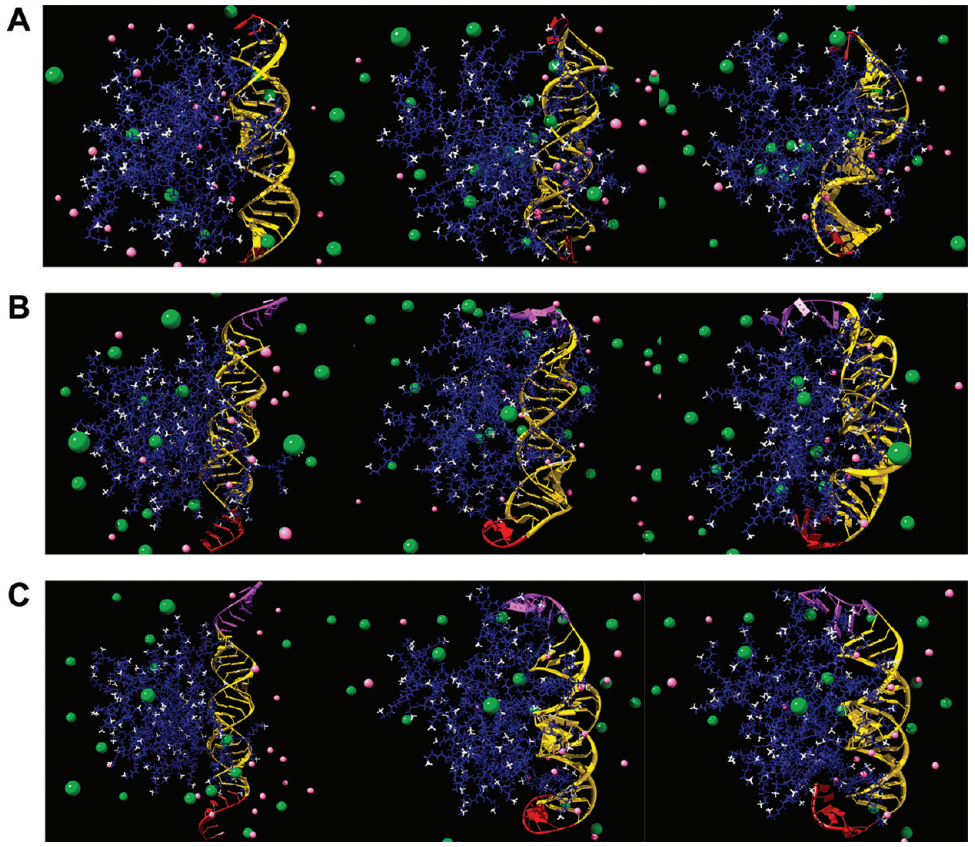

Figure 3. Molecular dynamics (MD) snapshots of the TEA-core dendrimer $\mathbf{G_5}$ in complex with siRNA molecules bearing T_2/T_2 overhangs (A), A_5/T_5 overhangs (B), and A_7/T_7 overhangs (C) at pH 7 and in the presence of 0.1 M NaCl. MD frames are taken after 10 ns (left column), 50 ns (middle column), and 100 ns (right column). In all panels, the dendrimer is portrayed as blue sticks, with the terminal groups highlighted as white sticks-and-balls. The siRNA double helix is depicted in a yellow ribbon-slab representation, with the T and A nucleotide overhangs highlighted in dark red purple, respectively. Na^+ and Cl^- ions are shown as hot pink and green spheres, respectively. Water is not shown for clarity.

Table 1. Free Energy of Binding between a TEA-Core PAMAM Dendrimer of Generation 5, G_5, and a siRNA with T_2/T_2, A_5/T_5, and A_7/T_7 Overhangs (Conventional siRNA and Sticky siRNAs), Respectively[a]

system	N	ΔH_{bind} (kcal/mol)	$-T\Delta S_{bind}$ (kcal/mol)	ΔG_{bind} (kcal/mol)	$\Delta H_{bind}/N$ (kcal/mol)	$-T\Delta S_{bind}/N$ (kcal/mol)	$\Delta G_{bind}/N$ (kcal/mol)
$\mathbf{G_5}$/siRNA (T_2/T_2 overhangs)	44	−571.1 ± 2.6	254.3 ± 4.3	−316.8 ± 5.0	−13.0 ± 0.1	5.8 ± 0.1	−7.2 ± 0.1
$\mathbf{G_5}$/sticky siRNA (A_5/T_5 overhangs)	50	−637.40 ± 2.8	250.0 ± 4.1	−387.4 ± 5.0	−12.7 ± 0.1	5.0 ± 0.1	−7.7 ± 0.1
$\mathbf{G_5}$/sticky siRNA (A_7/T_7 overhangs)	54	−690.2 ± 4.7	267.3 ± 5.3	−422.9 ± 7.1	−12.8 ± 0.1	5.0 ± 0.1	−7.8 ± 0.1

[a] ΔH_{bind}, $-T\Delta S_{bind}$, and ΔG_{bind} represent the enthalpy, entropy, and free energy of binding between the dendrimer and the different siRNA molecules. $\Delta H_{bind}/N$, $-T\Delta S_{bind}/N$, and $\Delta G_{bind}/N$ are the corresponding normalized thermodynamic quantities per charge on the siRNA (N).

(Figure 4A), whereas no obvious fluorescent signals could be detected in the absence of $\mathbf{G_5}$ (data not shown). This finding indicates that the effective cell uptake of sticky siRNAs was indeed mediated by the $\mathbf{G_5}$ as the delivery vector.

It should be noted that cellular uptake of nanoparticles with sizes around 50−3000 nm involves several pathways including macropinocytosis, clathrin-mediated endocytosis, caveolae-mediated endocytosis etc.[22−27] In order to understand which pathway was responsible for the observed uptake of sticky siRNA/$\mathbf{G_5}$ nanoparticles, we studied the uptake mechanism using specific inhibitors and biomarkers of various endocytic pathways. As can be seen in Figure 4B, a significant reduction in the cell uptake of sticky siRNA/$\mathbf{G_5}$ complexes was observed in the presence of cytochalasin D (a macropinocytosis inhibitor), while only a moderate inhibitory effect on cell uptake was detected when genistein (an inhibitor of the tyrosine kinase specifically involved in caveolae-mediated endocytosis) and chlorpromazine (a specific inhibitor of clathrin-mediated endocytosis) were applied, respectively. In addition, we observed conspicuous colocalization of the Alexa647 labeled sticky siRNA/$\mathbf{G_5}$ complexes with dextran (a macropinocytosis biomarker), whereas minor and moderate colocalization was detected with transferrin and cholera toxin B, biomarkers of clathrin- and caveolae-mediated endocytosis, respectively (Figure 4C). Furthermore, treatment with the sticky siRNA/$\mathbf{G_5}$ nanocomplexes led to significant actin depolymerization, a hallmark of macropinocytosis (Figure 4D). Collectively, these results clearly highlight macropinocytosis as the major uptake pathway, with clathrin- and caveolae-mediated endocytosis showing only partial involvement.

Potent and Specific Gene Silencing of Hsp27 and Anticancer Activity *in Vitro*. To further assess $\mathbf{G_5}$-mediated

dx.doi.org/10.1021/mp2006104 | *Mol. Pharmaceutics* 2012, 9, 470−481

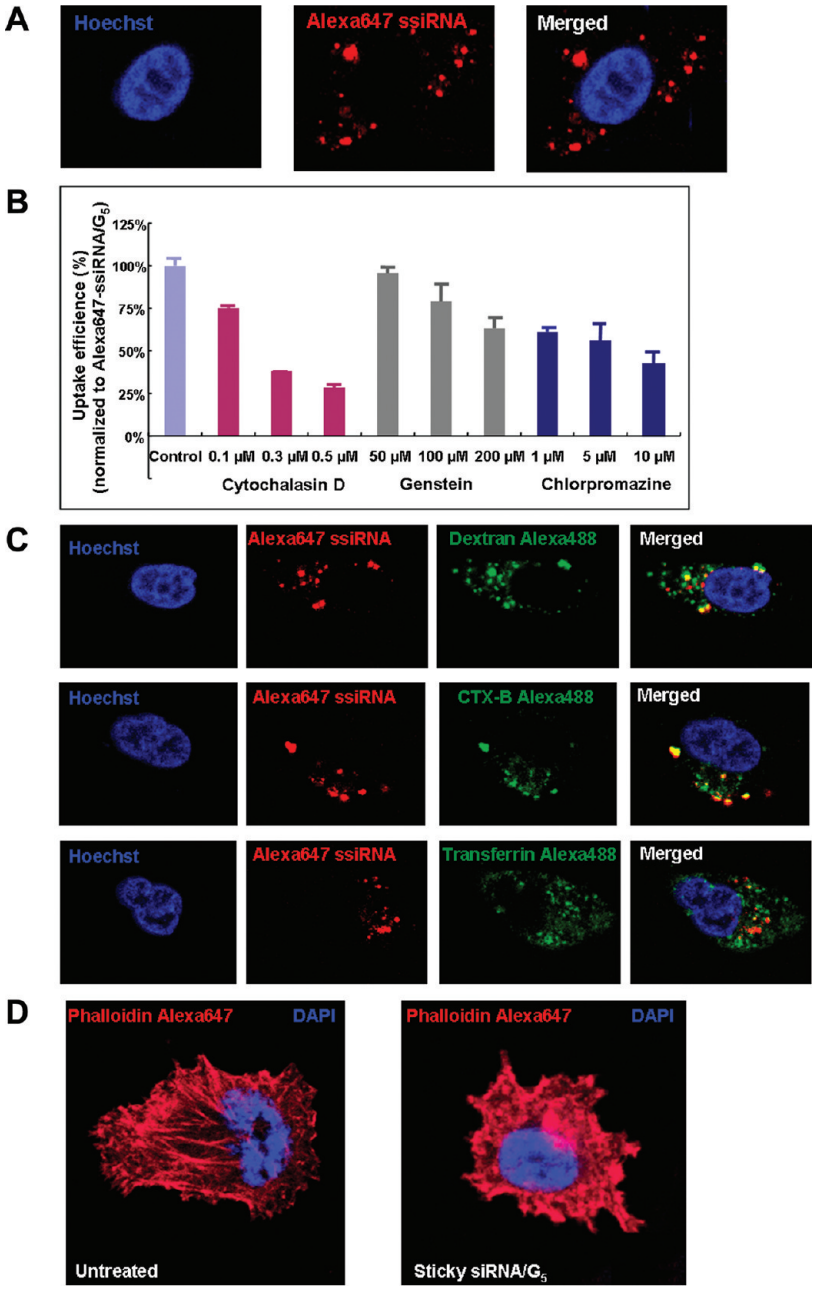

Figure 4. Uptake of Alexa647-labeled sticky siRNA/$\mathbf{G_5}$ complexes on PC-3 cells analyzed by live-cell confocal microscopy (A), using specific inhibitors (B) and fluorescent endocytic biomarkers (C) of different uptake pathways and phalloidin probe for actin rearrangement (D). (A) Blue channel image of the nuclei of PC-3 cells stained by Hoechst 34580 (left), red channel image of the Alexa647-labeled sticky siRNA/$\mathbf{G_5}$ nanoparticles (red), and merged image of both (right). (B) Effect of cytochalasin D (to inhibit macropinocytosis), genistein (to inhibit caveolae-mediated endocytosis) and chlorpromazine (to inhibit clathrin-mediated endocytosis) on the cell uptake of the Alexa647-labeled sticky siRNA/$\mathbf{G_5}$ complexes. (C) Colocalization of Alexa647-labeled sticky siRNA/$\mathbf{G_5}$ complexes with different endocytic markers: dextran (marker of macropinocytosis), cholera toxin B (marker of caveolae-mediated endocytosis) and transferrin (marker of clathrin-mediated endocytosis), green channel image of the Alexa488-labeled different endocytic biomarkers. (D) Fluorescent labeling of actin fibers using Alexa647-labeled phalloidin reveals actin depolymerization, a hallmark of macropinocytosis.

sticky siRNA delivery to target Hsp27 in prostate cancer PC-3 cells, we evaluated the efficiency and specificity of the gene silencing effect at both the mRNA and the protein level using qRT-PCR and Western blotting analysis, respectively. As shown in Figure 5A, the mRNA level of Hsp27 was significantly decreased after treatment with $\mathbf{G_5}$/sticky siRNA, relative to no decrease with either the dendrimer $\mathbf{G_5}$ alone or the scramble/$\mathbf{G_5}$ complex, using nontreatment as control. This efficient and specific downregulation of Hsp27 mRNA is attributed to the RNAi response after effective delivery of Hsp27 sticky siRNA mediated by $\mathbf{G_5}$. Likewise, compared to the nontreated control, the level of Hsp27 protein was almost completely suppressed following the treatment with $\mathbf{G_5}$/sticky siRNA (Figure 5B). The specificity of the downregulation of Hsp27 protein was also confirmed by comparing the inhibition results obtained with the dendrimer $\mathbf{G_5}$ alone, and the $\mathbf{G_5}$/scrambled sticky siRNA (Figure 5B).

dx.doi.org/10.1021/mp2006104 | *Mol. Pharmaceutics* 2012, 9, 470−481

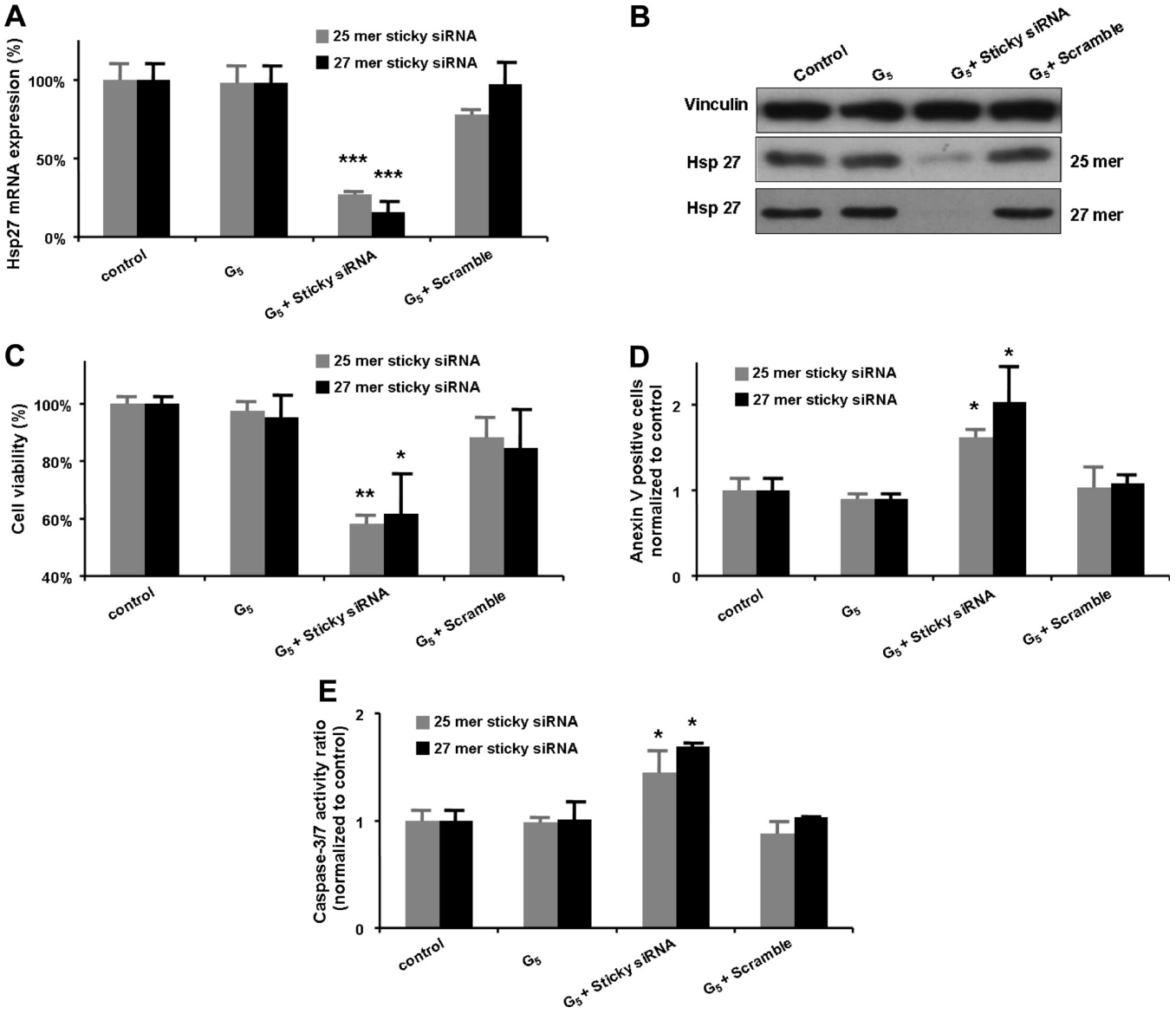

Figure 5. G_5/Hsp27 sticky siRNA mediated effective and specific gene silencing and anticancer activity in prostate cancer PC-3 cells. (A) Hsp27 mRNA expression assessed using quantitative real-time (qRT)-PCR 2 days post-treatment, with 18S ribosomal mRNA as reference. (B) Hsp27 protein expression quantified using Western blot 3 days post-treatment with vinculin as reference. Effect of Hsp27 gene silencing on (C) cell proliferation, (D) apoptosis and (E) caspase-3/7 activity after treatment with 50 nM Hsp27 sticky siRNA/$\mathbf{G_5}$ nanoparticles at an N/P ratio 10, relative to scramble/$\mathbf{G_5}$, $\mathbf{G_5}$ alone and no treatment controls. Cell proliferation was determined by MTT assay 6 days post-treatment. Apoptotic index was measured with FACS flow cytometry by annexin V assay 4 days post-treatment. Caspase-3/7 activity was detected using colormetric assay 3 days post-treatment. *, ** and ***, differ from control ($p \leq 0.05$, $p \leq 0.01$ and $p \leq 0.001$, respectively) by Student's t test.

Bearing in mind the vital regulatory role of Hsp27 in cell survival,[12,21] we next wished to investigate further the anticancer effect resulting from treatment with Hsp27 sticky siRNA/$\mathbf{G_5}$ complexes on PC-3 cells. We expected inhibition of Hsp27 expression to yield increased caspase-3 cleavage, apoptosis, and significant suppression of cell growth.[11,21,28] Using MTT assay, we observed a considerable inhibition of PC-3 cell proliferation after treatment with Hsp27 sticky siRNA/$\mathbf{G_5}$ compared to controls (nontreatment control and treatment with the dendrimer $\mathbf{G_5}$ alone or scramble/$\mathbf{G_5}$) (Figure 5C). We then measured the apoptosis-inducing activity using fluorescence activated cell sorting (FACS) flow cytometry. FACS flow analysis revealed a considerable increase of annexin V-positive apoptotic cells after treatment with Hsp27 sticky siRNA/$\mathbf{G_5}$, compared to controls (nontreatment control and treatment with the dendrimer $\mathbf{G_5}$ alone or scramble/$\mathbf{G_5}$) (Figure 5D). This would imply that the apoptosis induced by Hsp27 sticky siRNA/$\mathbf{G_5}$ treatment may represent the major mode of cell death. We further evaluated caspase activation, another hallmark of apoptosis, on PC-3 cells. As can be seen in Figure 5E, compared to control (nontreatment, dendrimer $\mathbf{G_5}$ alone or scramble/$\mathbf{G_5}$), there was a notable increase in caspase-3/7 activity following Hsp27 sticky siRNA/$\mathbf{G_5}$ treatment, suggesting a caspase-3/7-dependent mechanism of apoptosis induction. Finally, we evaluated the toxicity of our delivery system using both MTT and lactate dehydrogenase (LDH) cytotoxicity assays. No considerable toxicity of $\mathbf{G_5}$-mediated sticky siRNA delivery was detected in PC-3 cells (Figure S3 in the Supporting Information), demonstrating its strong potential for further *in vivo* application.

dx.doi.org/10.1021/mp2006104 | *Mol. Pharmaceutics* 2012, 9, 470−481

Effective Delivery of Sticky siRNA and Potent Gene Silencing of Hsp27 *in Vivo*. We next evaluated the *in vivo* gene silencing capacity using a prostate cancer PC-3 xenografted nude mouse model. Hsp27 sticky siRNA/$\mathbf{G_5}$ complexes were slowly injected via intratumoral administration. All mice survived well during and after the intervention, and no sign of toxicity was observed. Mice were sacrified after one week of treatment, and the expression of Hsp27 mRNA and protein in the tumors was measured by qRT-PCR and Western blotting, respectively. Significant downregulation of Hsp27 at both the mRNA (Figure 6A) and protein (Figure 6B) levels was observed with Hsp27 sticky siRNA/$\mathbf{G_5}$, compared to the controls (PBS buffer-treated control and treatment with the dendrimer $\mathbf{G_5}$ alone or the scrambled siRNA/$\mathbf{G_5}$). These data indicate that Hsp27 sticky siRNA retains its ability to induce a potent and specific RNAi response *in vivo* after $\mathbf{G_5}$-mediated intratumoral delivery.

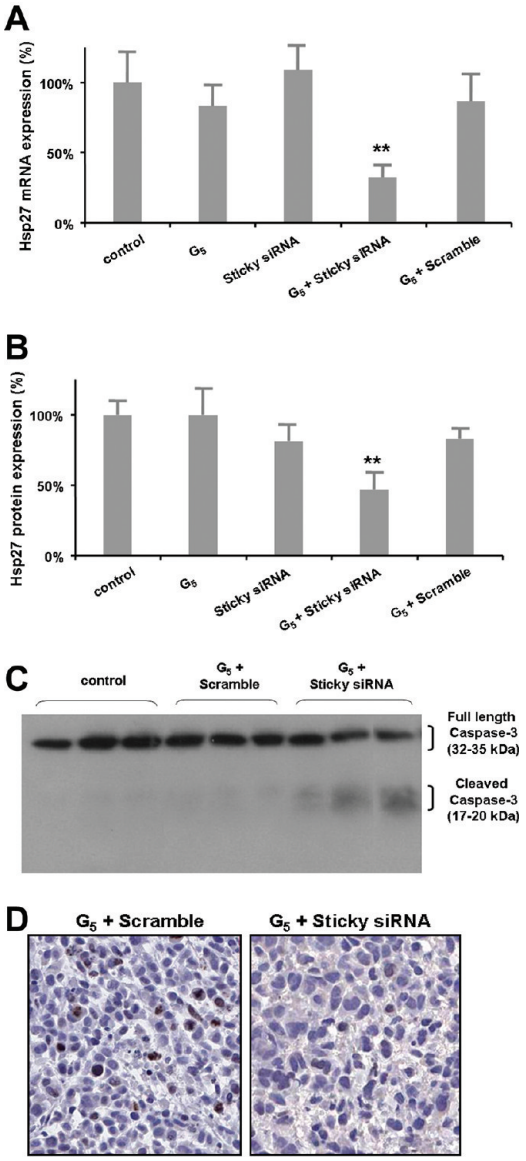

Figure 6. Effective and specific gene silencing of Hsp27, caspase activation and antiproliferative effect in the PC-3 cell xenografted nude mice after intratumoral injection of Hsp27 sticky siRNA/$\mathbf{G_5}$ complex, related to PBS buffer, $\mathbf{G_5}$ alone, Hsp27 sticky siRNA alone and scramble/$\mathbf{G_5}$ as controls. Downregulation of Hsp27 at both mRNA (A) and protein (B) levels was achieved after 1 week of treatment. (C) Caspase activation was measured by Western blot assay and (D) evaluation of tumor cell proliferation *via* immunohistochemistry using Ki-67 staining. ** differ from control ($p \leq 0.01$) by Student's *t* test.

We also assessed the caspase activation and antiproliferation activity *in vivo*. Using Western blot with an anti-caspase-3 antibody that recognizes both full-length (32−35 kDa) and cleaved caspase-3 (17−20 kDa), we observed the active cleaved caspase-3 fragments only in mice treated with Hsp27 sticky siRNA/$\mathbf{G_5}$ (Figure 6C). Further immunohistochemistry results with Ki-67 antibody staining confirmed the considerable inhibition of cell proliferation in mice treated with Hsp27 sticky siRNA/$\mathbf{G_5}$ compared with scrambled siRNA/$\mathbf{G_5}$ (Figure 6D). Collectively, our results demonstrate that the $\mathbf{G_5}$ dendrimer is a safe nanovector which can be used for *in vivo* sticky siRNA delivery leading to effective gene silencing, caspase activation and antiproliferation effects, as shown in our prostate cancer PC-3 xenografted nude mouse model.

CONCLUSION

In our quest for safe and efficient vectors for the delivery of siRNA therapeutics, we have discovered that a TEA-core PAMAM dendrimer of generation 5 is effective at delivering sticky siRNAs targeting Hsp27, resulting in potent gene silencing and promising anticancer effects in a prostate cancer model both *in vitro* and *in vivo*. Prostate cancer is one of the most common cancers and is a leading cause of cancer death in men in industrialized countries.[29] While most prostate cancer patients initially respond to first-line hormonal therapy, many become refractory to hormonal and other traditional therapies, ultimately leading to castration-resistant prostate cancer for which there is no effective treatment available to date. Targeting Hsp27, a molecular chaperone involved in drug resistance, with siRNA therapeutic molecules is emerging as an attractive novel strategy for treating prostate cancer,[11,12] provided that safe and efficient siRNA delivery vectors are made available.[13]

We have previously demonstrated that a structurally flexible TEA-core PAMAM dendrimer of generation 7 is effective at delivering siRNAs targeting Hsp27 in a prostate cancer model.[8] However, the large-scale chemical synthesis of this higher generation dendrimer with good quality is technically demanding, and it would be potentially difficult to meet the purity and quality control standards required by clinical applications. We therefore wished to develop lower generation dendrimers as efficient siRNA delivery vectors. In the present work, we have shown that by using sticky siRNA molecules with complementary A_n/T_n overhangs (n = 5 or 7), the lower generation $\mathbf{G_5}$ TEA-core PAMAM dendrimer can effectively deliver siRNA to achieve potent gene silencing of Hsp27 and significant anticancer activity in the prostate cancer PC-3 cell model *in vitro* and *in vivo*.

Noteworthy is the unique advantage offered by the complementary A_n/T_n overhangs in the sticky siRNAs. These overhangs can self-assemble to form "gene-like" longer double stranded RNA molecules[14] leading to a stronger cooperativity and efficient interactions with small or low generation dendrimers. We further showed in this study, in contrast to the shorter T_2/T_2 overhangs in conventional siRNA, the relatively longer A_n/T_n overhangs in sticky siRNA may also favor the interaction with smaller dendrimers. Such overhangs may act as two "molecular arms" embracing the dendrimeric vector enabling a better interaction, stronger binding and improved delivery efficiency of these low generation nanovectors. Last but not least, recent study

demonstrated that, similar to siRNA, sticky siRNA molecules did not induce immune response,[30] although they have the capacity to reversibly assemble into "gene-like" longer double stranded RNA molecules.

Finally, low generation dendrimers such as G_5 shown here as effective vectors for siRNA therapeutics will certainly prove to be a technical advantage for further translational research involving the combination of sticky siRNAs with G_5 in siRNA-based therapeutic approaches. Not only will the synthesis of the low generation dendrimer G_5 be more precisely controlled compared to that of its G_7 counterpart, but its molecular characterization and quality control will be greatly facilitated. This will undoubtedly promote further development of siRNA-based therapeutic interventions in combination with our dendrimers to treat cancer and other major human diseases. We foresee a fueled interest in this direction in the near future.

■ ASSOCIATED CONTENT

Supporting Information

Experimental details, table of size and zeta potential of sticky siRNA/G_5 complexes, and additional figures. This material is available free of charge via the Internet at http://pubs.acs.org.

■ AUTHOR INFORMATION

Corresponding Author

*Centre Interdisciplinaire de Nanoscience de Marseille, CNRS UMR 7325, Département de Chimie, 163 avenue de Luminy, 13288 Marseille cedex 09, France. Tel: (33) 4 91829154. Fax: (33) 4 91829301. E-mail: ling.peng@univmed.fr.

■ ACKNOWLEDGMENTS

This work was supported by the international ERA-Net EURONANOMED European Research project DENANORNA, National Natural Science Foundation of China (No. 20572081), National Mega Project on Major Drug Development (No. 2009ZX0930-014), Association Française contre les Myopathies (No. 13074, 10793), Wuhan University, CNRS, INSERM and under the auspices of European COST Action TD0802 "Dendrimers in Biomedical Applications". We thank Dr. Jiehua Zhou for her critical comments and careful reading of the manuscript, and Mr. Qi Wang for his help with some figures. We are grateful to Dr. Juan L. Iovanna for his kind interest and hospitality during the performance of this work.

■ ABBREVIATIONS USED

siRNA, small-interfering RNA; TEA, triethanolamine; PAMAM, poly(amidoamine); G, dendrimer generation; Hsp27, heat shock protein 27; ssiRNA, sticky siRNA; PEI, polyethylenimine; BSA, bovine serum albumin; DAPI, 4′,6′-diamidino-2-phenylindole; FBS, fetal bovine serum; qRT-PCR, quantitative real-time polymer chain reaction; MTT, 3-(4,5-dimethylthiazol-2-yl)-2,5-diphenyl tetrazolium bromide; 7-AAD, 7-aminoactinomycin D; FACS, fluorescence activated cell sorting; lactate dehydrogenase (LDH); DAB, diaminobenzidine; DPX, distyrene plasticizer xylene; MM/PBSA, molecular mechanics/Poisson−Boltzmann surface area

■ REFERENCES

(1) de Fougerolles, A.; Vornlocher, H. P.; Maraganore, J.; Lieberman, J. Interfering with disease: a progress report on siRNA-based therapeutics. *Nat. Rev. Drug Discovery* **2007**, *6*, 443−453.

(2) Castanotto, D.; Rossi, J. J. The promises and pitfalls of RNA-interference-based therapeutics. *Nature* **2009**, *457*, 426−433.

(3) Davidson, B. L.; McCray, P. B. Jr. Current prospects for RNA interference-based therapies. *Nat. Rev. Genet.* **2011**, *12*, 329−340.

(4) Whitehead, K. A.; Langer, R.; Anderson, D. G. Knocking down barriers: advances in siRNA delivery. *Nat. Rev. Drug Discovery* **2009**, *8*, 129−138.

(5) Wu, J.; Zhou, J.; Qu, F.; Bao, P.; Zhang, Y.; Peng, L. Polycationic dendrimers interact with RNA molecules: polyamine dendrimers inhibit the catalytic activity of Candida ribozymes. *Chem. Commun. (Cambridge, U.K.)* **2005**, 313−315.

(6) Liu, X. X.; Wu, J. Y.; Yamine, M.; Zhou, J. H.; Posocco, P.; Viel, S.; Liu, C.; Ziarrelli, F.; Fermeglia, M.; Pricl, S.; Vicotrero, G.; Nguyen, C.; Erbacher, P.; Behr, J.-P.; Peng, L. Structurally flexible triethanolamine core PAMAM dendrimers are effective nanovectors for DNA transfection in vitro and in vivo to the mouse thymus. *Bioconjugate Chem.* **2011**, *22*, 2461−2473.

(7) Zhou, J.; Wu, J.; Hafdi, N.; Behr, J. P.; Erbacher, P.; Peng, L. PAMAM dendrimers for efficient siRNA delivery and potent gene silencing. *Chem. Commun. (Cambridge, U.K.)* **2006**, 2362−2364.

(8) Liu, X. X.; Rocchi, P.; Qu, F. Q.; Zheng, S. Q.; Liang, Z. C.; Gleave, M.; Iovanna, J.; Peng, L. PAMAM dendrimers mediate siRNA delivery to target Hsp27 and produce potent antiproliferative effects on prostate cancer cells. *ChemMedChem* **2009**, *4*, 1302−1310.

(9) Zhou, J.; Neff, C. P.; Liu, X.; Zhang, J.; Li, H.; Smith, D. D.; Swiderski, P.; Aboellail, T.; Huang, Y.; Du, Q.; Liang, Z.; Peng, L.; Akkina, R.; Rossi, J. J. Systemic Administration of Combinatorial dsiRNAs via Nanoparticles Efficiently Suppresses HIV-1 Infection in Humanized Mice. *Mol. Ther.* **2011**, *19*, 2228−2238.

(10) Liu, X. X.; Rocchi, P.; Peng, L. Dendrimers as non-viral vectors for siRNA delivery. *New J. Chem.* **2012**, *36*, 256−263.

(11) Cornford, P. A.; Dodson, A. R.; Parsons, K. F.; Desmond, A. D.; Woolfenden, A.; Fordham, M.; Neoptolemos, J. P.; Ke, Y.; Foster, C. S. Heat shock protein expression independently predicts clinical outcome in prostate cancer. *Cancer Res.* **2000**, *60*, 7099−7105.

(12) Rocchi, P.; So, A.; Kojima, S.; Signaevsky, M.; Beraldi, E.; Fazli, L.; Hurtado-Coll, A.; Yamanaka, K.; Gleave, M. Heat shock protein 27 increases after androgen ablation and plays a cytoprotective role in hormone-refractory prostate cancer. *Cancer Res.* **2004**, *64*, 6595−6602.

(13) Stavridi, F.; Karapanagiotou, E. M.; Syrigos, K. N. Targeted therapeutic approaches for hormone-refractory prostate cancer. *Cancer Treat. Rev.* **2010**, *36*, 122−130.

(14) Bolcato-Bellemin, A. L.; Bonnet, M. E.; Creusat, G.; Erbacher, P.; Behr, J. P. Sticky overhangs enhance siRNA-mediated gene silencing. *Proc. Natl. Acad. Sci. U.S.A.* **2007**, *104*, 16050−16055.

(15) Boussif, O.; Lezoualc'h, F.; Zanta, M. A.; Mergny, M. D.; Scherman, D.; Demeneix, B.; Behr, J. P. A versatile vector for gene and oligonucleotide transfer into cells in culture and in vivo: polyethylenimine. *Proc. Natl. Acad. Sci. U.S.A.* **1995**, *92*, 7297−7301.

(16) Shen, X. C.; Zhou, J.; Liu, X.; Wu, J.; Qu, F.; Zhang, Z. L.; Pang, D. W.; Quelever, G.; Zhang, C. C.; Peng, L. Importance of size-to-charge ratio in construction of stable and uniform nanoscale RNA/dendrimer complexes. *Org. Biomol. Chem.* **2007**, *5*, 3674−3681.

(17) Case, D. A.; Darden, T. A.; Cheatham, T. E., III; Simmerling, C. L.; Wang, J.; Duke, R. E.; Luo, R.; Merz, K. M.; Pearlman, D. A.; Crowley, M.; Walker, R. C.; Zhang, W.; Wang, B.; Hayik, S.; Roitberg, A.; Seabra, G.; Wong, K. F.; Paesani, F.; Wu, X.; Brozell, S.; Tsui, V.; Gohlke, H.; Yang, L.; Tan, C.; Mongan, J.; Hornak, V.; Cui, G.; Beroza, P.; Mathews, D. H.; Schafmeister, C.; Ross, W. S.; Kollman, P. A. *AMBER 9*; University of California: San Francisco, CA, USA, 2006.

(18) Posocco, P.; Pricl, S.; Jones, S.; Barnard, A.; Smith, D. K. Less is more − multiscale modelling of self-assembling multivalency and its impact on DNA binding and gene delivery. *Chem. Sci.* **2010**, *1*, 393−404.

(19) Pavan, G. M.; Posocco, P.; Tagliabue, A.; Maly, M.; Malek, A.; Danani, A.; Ragg, E.; Catapano, C. V.; Pricl, S. PAMAM dendrimers for siRNA delivery: computational and experimental insights. *Chem.—Eur. J.* **2011**, *16*, 7781−7795.

(20) Srinivasan, J.; Cheatham, T. E.; Cieplak, P.; Kollman, P. A.; Case, D. A. Continuum Solvent Studies of the Stability of DNA, RNA,

and phosphoramidate DNA helices. *J. Am. Chem. Soc.* **1998**, *120*, 9401−9409.
(21) Rocchi, P.; Beraldi, E.; Ettinger, S.; Fazli, L.; Vessella, R. L.; Nelson, C.; Gleave, M. Increased Hsp27 after androgen ablation facilitates androgen-independent progression in prostate cancer via signal transducers and activators of transcription 3-mediated suppression of apoptosis. *Cancer Res.* **2005**, *65*, 11083−11093.
(22) Huth, U. S.; Schubert, R.; Peschka-Suss, R. Investigating the uptake and intracellular fate of pH-sensitive liposomes by flow cytometry and spectral bio-imaging. *J. Controlled Release* **2006**, *110*, 490−504.
(23) Manunta, M.; Nichols, B. J.; Tan, P. H.; Sagoo, P.; Harper, J.; George, A. J. Gene delivery by dendrimers operates via different pathways in different cells, but is enhanced by the presence of caveolin. *J. Immunol. Methods* **2006**, *314*, 134−146.
(24) Midoux, P.; Breuzard, G.; Gomez, J. P.; Pichon, C. Polymer-based gene delivery: a current review on the uptake and intracellular trafficking of polyplexes. *Curr. Gene Ther.* **2008**, *8*, 335−352.
(25) Perumal, O. P.; Inapagolla, R.; Kannan, S.; Kannan, R. M. The effect of surface functionality on cellular trafficking of dendrimers. *Biomaterials* **2008**, *29*, 3469−3476.
(26) Saovapakhiran, A.; D'Emanuele, A.; Attwood, D.; Penny, J. Surface modification of PAMAM dendrimers modulates the mechanism of cellular internalization. *Bioconjugate Chem.* **2009**, *20*, 693−701.
(27) Seib, F. P.; Jones, A. T.; Duncan, R. Comparison of the endocytic properties of linear and branched PEIs, and cationic PAMAM dendrimers in B16f10 melanoma cells. *J. Controlled Release* **2007**, *117*, 291−300.
(28) Rocchi, P.; Jugpal, P.; So, A.; Sinneman, S.; Ettinger, S.; Fazli, L.; Nelson, C.; Gleave, M. Small interference RNA targeting heat-shock protein 27 inhibits the growth of prostatic cell lines and induces apoptosis via caspase-3 activation in vitro. *BJU Int.* **2006**, *98*, 1082−1089.
(29) Jemal, A.; Siegel, R.; Xu, J.; Ward, E. Cancer statistics, 2010. *CA—Cancer J. Clin.* **2010**, *60*, 277−300.
(30) Bonnet, M. E.; Erbacher, P.; Bolcato-Bellemin, A. L. Systemic delivery of DNA or siRNA mediated by linear polyethylenimine (L-PEI) does not induce an inflammatory response. *Pharm. Res.* **2008**, *25*, 2972−2982.